Experiential Integral Backstepping Sliding Mode Controller to achieve the Maximum Power Point of a PV system

Brahim Khalil Oubbati, Mohamed Boutoubat, Abdelhamid Rabhi, Mohammed Belkheiri

Experiential Integral Backstepping Sliding Mode Controller to Achieve the Maximum Power Point of a PV System

Brahim Khalil Oubbati[a,c], Mohamed Boutoubat[b], Abdelhamid Rabhi[c], Mohamed Belkheiri[a]

[a] *University of Laghouat, LTSS Lab. Laghouat, Algeria*
[b] *University of Laghouat, LACoSERE Lab. Laghouat, Algeria*
[c] *University of Picardie ,MIS Lab,Amiens, France*

Abstract

Maximum Power Point Tracking (MPPT) strategy is necessary to extract the maximum power production of a Photovoltaic (PV) system. Since the PV has nonlinear dynamics, it is more suitable to use a nonlinear MPPT controller to improve the tracking efficiency. The modelling and control of most systems in real-time are not fully precise and introduce some variations such as : the steady state error and ripples in the system outputs. In this paper, a classical sliding mode controller has been designed and applied experimentally to the PV system to achieve the Maximum Power Point (MPP). The results show that the system responses present chattering phenomena with no negligible state error. In order to reduce these drawbacks (chattering and steady-state error), an Integral Backstepping combined with a discontinuous Sliding Mode Controller (IBSMC) is proposed and applied experimentally to the PV system. The obtained experimental results for the two controllers are compared under the same weather conditions, in terms of chattering phenomena and state error. As a result, the proposed hybrid controller (IBSMC) has achieved high dynamic system performances. Moreover, the stability of this system has been proved using Lyapunov stability criteria.

Keywords: Integral Backstepping Sliding Mode Control (IBSMC), PV, MPPT, Lyapunov criteria, Sliding Mode Control (SMC).

1. Introduction

Recently, the power produced by Photovoltaic (PV) systems has gained worldwide popularity for many reasons such as: the decrease of fossil fuels (gas and oil. . .), their abundant availability, and their eco-friendly aspect [1].

Email addresses: i.oubbati@lagh-univ.dz (Brahim Khalil Oubbati), boutoubat90@yahoo.fr (Mohamed Boutoubat), abdelhamid.rabhi@u-picardie.fr (Abdelhamid Rabhi)

Besides, the generated PV power magnitude depends mainly on the variation of the weather conditions such as the temperature, humidity, and the amount of the received global solar radiations. Moreover, the choice of the controller's types has also its effect on the system responses, more precisely in the MPPT mode [2].

Generally, the term MPPT refers to the maximum power point tracking controller that is necessary to force a PV system to operate at its maximum power point. Nowadays, many MPPT techniques ranged from conventional and unconventional approaches has been proposed. the methods proposed in the literature, and that guarantee the maximum power produced from PV panels, could be categorise as follow :

First, the conventional control algorithms such as: incremental conductance [3], fractional short circuit current, open-circuit voltage, and Perturb an Observe (P&O)[4, 5], achieve the maximum point based on the P-V characteristic curve. In addition, hill-climbing algorithms are based on introducing a net, negative or positive (increase or decrease) values. However, the main issue of these algorithms is the system response fluctuations (produced power, load current...). Even if the Maximum Power Point (MPP) is achieved, and by a consequence, the overall system will lose its efficiency and power quality.

The second important category, namely ; Meta-Heuristic optimization techniques such as Salp Swarm algorithm (SSA), Grey wolf optimization (GWO), Genetic Algorithm (GA), Particle Swarm Optimization (PSO) and Ant Colony Optimization (ACO) [6, 7, 8, 9, 10] have been efficiently tested to search the maximum Power Point under partial shading conditions. Generally, they use the same procedure to optimize the maximum Power Point. Their efficiency depends strongly on the population of different individuals, from which each individual can represent a solution. A minimization process between each individual and their parents using a cost function is done for each iteration in order to achieve the best goal. The main advantage of these algorithms is that the chance of reaching the MPPT is very high [11].

Moreover, other algorithms category which are widely used in the case of a shaded PV systems are the Artificial Intelligent AI and fuzzy logic controllers for MPPT applications [12]. In [13], an Artificial Neural Network (ANN) is used to detect the region containing the global MPP. After that, the P&O algorithm is introduced to find the optimum point of the maximum power. However, these algorithms decrease the system efficiency and are known by their implementation complexity [14]. On the other hand, fuzzy logic based control methods can do it better thanks to their short

response time to reach the MPP [15, 16, 17] . However, the performances of theses systems depends strongly on logic condition (IF-Else) law bases.

Consequently, many works have studied a different kind of MPPT strategies. From literature, we distinguish to main techniques. The first one is called a voltage-oriented MPPT (VO-MPPT) in cascade with a voltage controller, and the second one is called a current-oriented MPPT (CO-MPPT) in cascade with a current controller. In this case, the previous mentioned techniques such as: P&O,INC . . . ., will be used to generate the reference value (either current or voltage reference).

Based on this review, linear controllers strategies can improve the efficiency of the system to find the MPP. The aim of using linear controllers is to adjust accurately the required MPPT duty cycle which improves the dynamic system performances. However, the controller's performance depends entirely on their selected parameters in order to produce the maximum power. These parameters can be enhanced using optimization methods such as genetic algorithms, which are used for PID controller parameters optimization in [18]. Other linear control algorithms can be found such as Ziegler Nichols tuning method used to determine the optimal gain of PID controller to improve the P&O-MPPT performance of grid connected PV system [19]. However, despite the main advantages of linear controllers to solve the MPPT problems, they are not able to reduce the state error and ripples.

This stability problem is due essentially to the nonlinear nature of the PV system. Linearization methods are proposed to model the converters with the assumption that they respond linearly to the varying duty cycle. However, they also experience nonlinear behaviour. Hence, as a solution, nonlinear controllers are introduced in several researches such as the backstepping and sliding mode control [20, 21, 22, 23, 24, 25, 26]. They are used to track the MPP of PV modules. The main advantage of these controllers is the robustness and stability of the overall system while tracking the MPP. However, the main drawbacks of such techniques are the important steady-state error and chattering phenomena.

There are many sliding mode controllers that have been designed to cope with the steady-state error and chattering phenomenon. The traditional SMC with an integral action added to the sliding surface (ISMC) is proposed in [27]. The proposed ISMC has been compared with traditional SMC in terms of reducing the steady-state error. This controller offers a fixed frequency operating through PWM-based control. Nevertheless, chattering phenomenon and overshoot has been observed by using this controller (ISMC). Other works have added another integral action

term to the sliding surface (double integral) as illustrated in [28], in order to more reduce the steady-state error. This controller has achieved more minimization in the steady-state error. However, the amount of the overshooting increased considerably.

In [29], the authors have proposed an adaptive integral derivative sliding mode (AIDSM) controller to eliminate the overshoot and minimize the steady-state fluctuation. The implementation of this controller by using the Hardware-in-loop (HIL) has performed a good performance in terms of eliminating the overshoot and the steady-state fluctuation. This controller has been compared with the conventional P&O method.

Generally, the main drawbacks associated with the SMC family is that, in the case of implementing the rth-order sliding mode controller, the SMC needs knowledge of $S, \dot{S}, \ddot{S}..., S^{(r-1)}$ nd and high implementation complexity.

In [30], a backstepping controller with integral action has been proposed to extract the maximum power produced from the PV system. This controller is very efficient and robust, but its performance depends totally on the system modelling accuracy. Additionally, in their contribution, the authors used a non-inverting buck-boost as an interface between the PV system and load, which leads to a complex system model. Furthermore, the authors have assessed the controller performances by simulation without any experimental results.

The principal objective of this paper is to alleviate these drawbacks using a proposed integral backstepping sliding mode controller (IBSMC). This controller is based on a combination of an integral backstepping and a discontinuous classical sliding mode controller. The proposed controller has been verified firstly by simulation tests using Matlab/Simulink software, in order to evaluate the ability of this controller to respond under fast irradiation condition changing, robustness and performance. Secondly, the performances of this controller (IBSMC) have been compared experimentally with traditional sliding mode in terms of reducing the steady-state error and the chattering phenomenon. The scheme of the global studied system is shown in Fig.1.

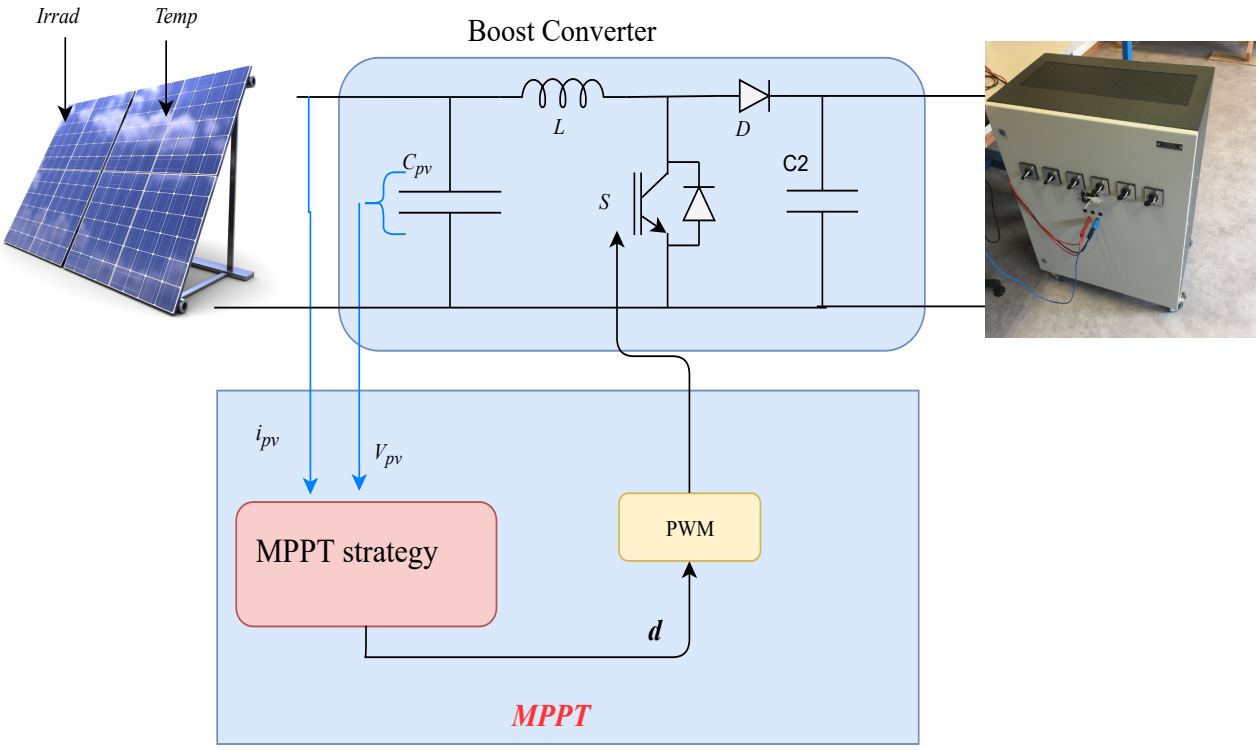

Figure 1: Global system scheme.

2. System modelling

2.1. PV system modelling

Photovoltaic system modelling is amply detailed in literature [31]. Hence, in this paper, we will present only the main equations that describe its electrical behavior.

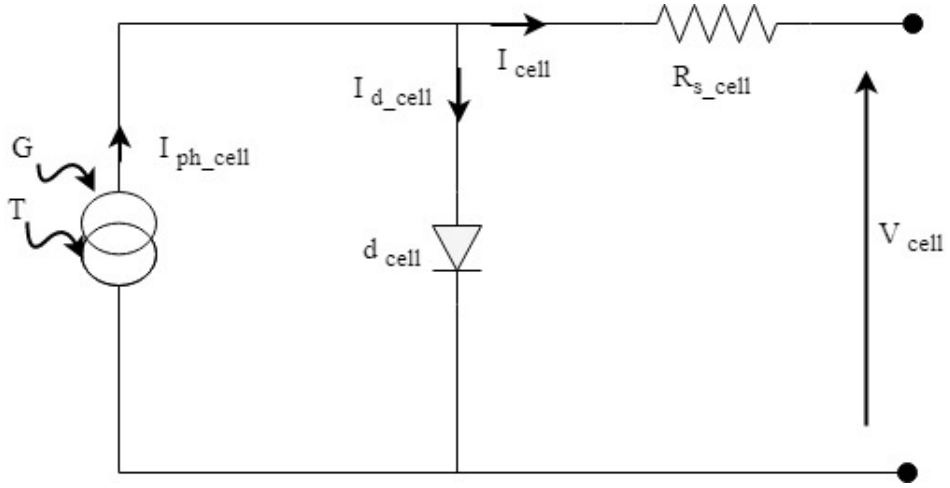

Figure 2: Equivalent PV circuit system based on the ohmic losses.

The output current of this module is given by:

$$i_{pv} = I_{ph\_cell} N_p M_p - N_p M_p I_0|_T \exp\left(\frac{\frac{v_M}{N_s M_s} + R_{cell}\frac{I_M}{N_p M_p}}{n_{pn} k_b \frac{T}{q}}\right) \tag{1}$$

2.2. Boost converter modelling

Generally, the main role of using the DC-DC boost converter is to push the PV system to produce the maximum power to the load. The differential classical equations expressed the dynamics of the boost converter are given as follows [32]:

$$\begin{cases} L\frac{di}{dt} = -(1-d)V_c + V_{pv} \\ C\frac{dV_c}{dt} = (1-d)i_L - \frac{V_c}{R} \end{cases} \tag{2}$$

Using the average mode over one switching period and assuming x_1, x_2 and d to be an average value of i_L , V_c and u , which are defined as follows:

$$\begin{cases} x_1 = \langle i_L \rangle \\ x_2 = \langle V_c \rangle \\ u = \langle d \rangle \end{cases} \tag{3}$$

So, Eq.(2) takes the following form:

$$\begin{cases} \dot{x}_1 = -\frac{(1-u)}{L}x_2 + \frac{V_{pv}}{L} \\ \dot{x}_2 = \frac{(1-u)}{C}x_1 - \frac{x_2}{RC} \end{cases} \tag{4}$$

This averaged state-space model will be used to the design different controllers (integral backstepping sliding mode and classical sliding mode) considered in this paper.

3. Different MPPT controllers design

3.1. Proposed integral backstepping sliding mode controller design

The controller is based on the combination of an integral backstepping and a discontinuous sliding mode. Its control scheme is shown in Fig.3. In fact, to achieve the MPP for the PV panel, the structured scheme of this controller is based principally on two loops; the first one is based on a simple conventional method P&O to generate the reference value of the MPPT-PV current (I_{pv-ref}). For more smoothing the required MPPT duty cycle form, a second control loop based on a nonlinear IBSM controller is proposed to regulate the instantaneous PV current I_{pv} to its

reference MPPT value I_{pv-ref} and achieve consequently a smooth and an accurate MPPT duty cycle value of the boost converter. As a result, a smooth output PV power is produced to the load with improved power quality.

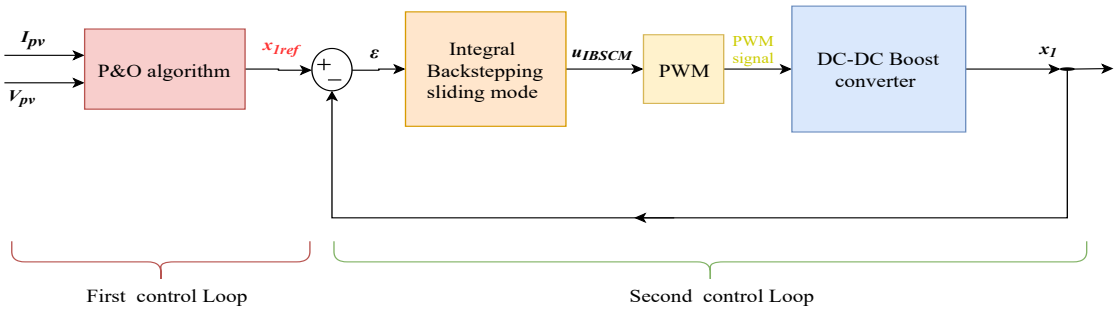

Figure 3: The global proposed closed-loop system control.

The flowchart of the proposed controller algorithm is depicted in Fig.4.

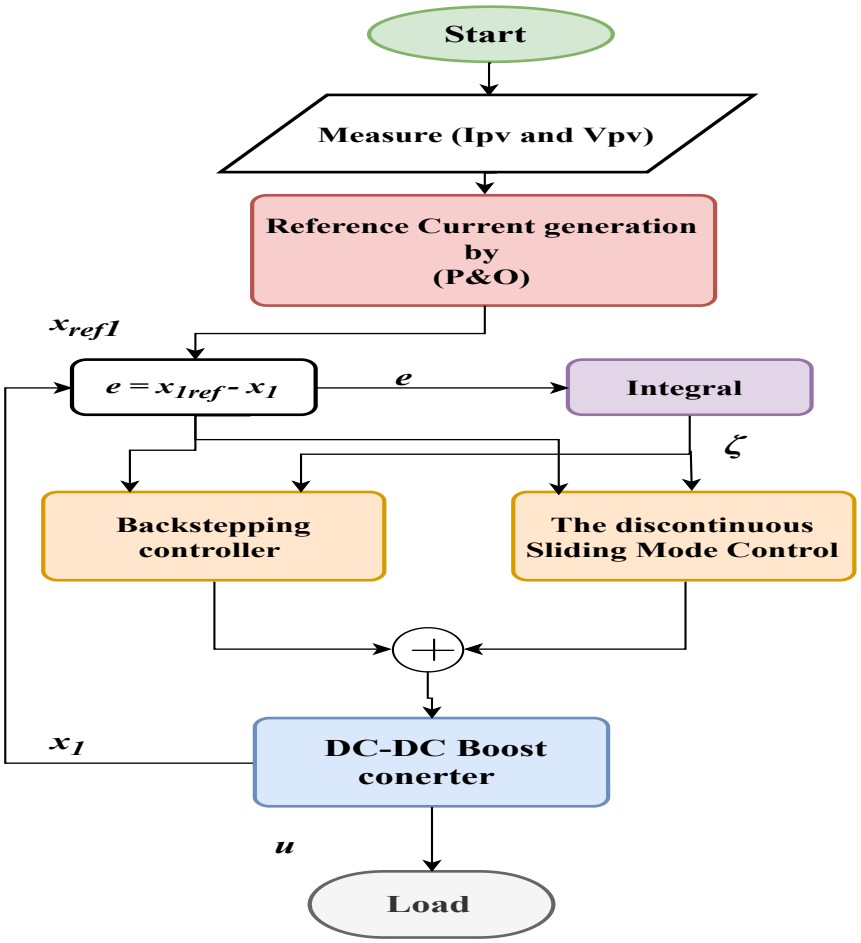

Figure 4: IBSMC proposed algorithm.

3.2. Reference MPPT PV current generated by a classical method (P&O)

Known as the featuring effective and simplicity of the classical P&O technique. Hence, it is more suitable to generate the reference MPPT value of the PV current (which corresponds to the maximum peak of the PV power). The flowchart of P&O algorithm is shown in Fig.5.

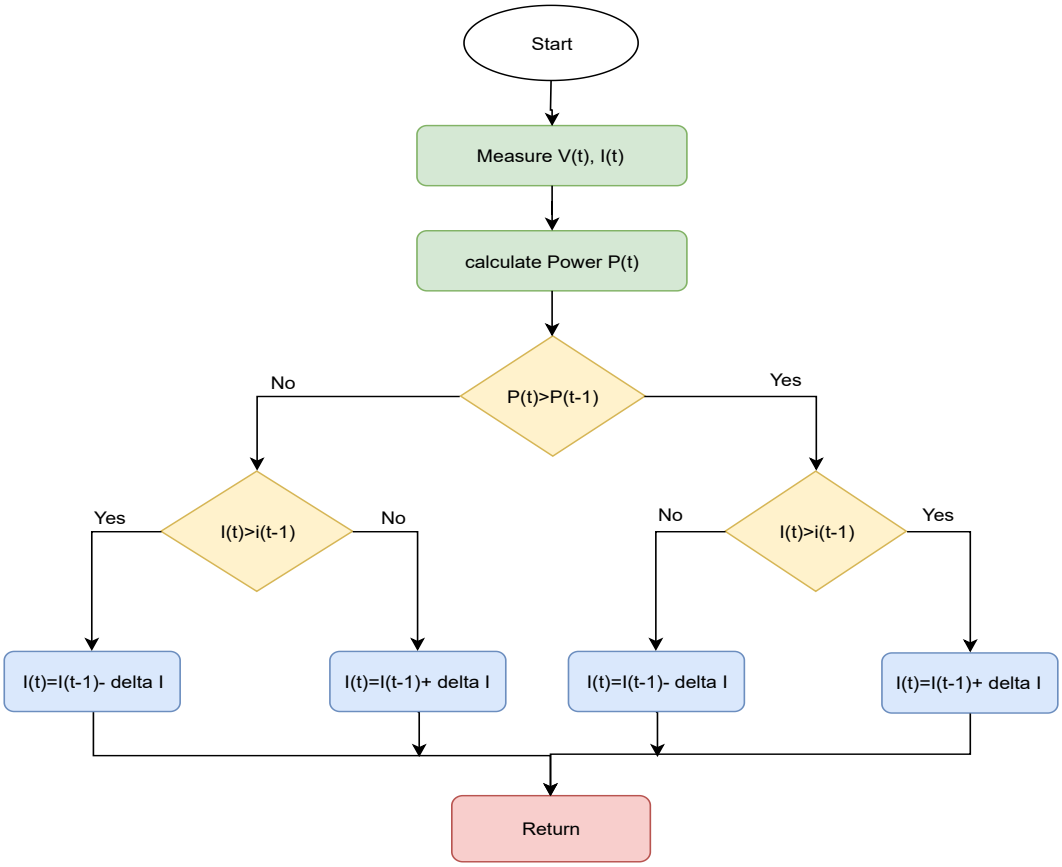

Figure 5: P&O algorithm.

3.3. Integral backstepping sliding mode control

In this paper, a nonlinear backstepping sliding mode structure is enhanced by introducing an integral action and a discontinuous sliding mode term in order to minimize the actual PV current error between the output PV current and its reference MPPT current(I_{pv-ref}) and to reduce the chattering ripples. The main role of the IBSM controller is to produce a smooth and an accurate duty cycle command value of the boost converter using the PV-MPPT current reference (I_{pv-ref}) value in order to force the PV system to track the maximum power point (MPPT) with a minimal state error and reduced chattering phenomena. The controller structure (see Fig. 4) contains

the reference MPPT current (I_{pv-ref}) generated by classical method (P&O).Then, Based on the error of the PV current and its MPPT reference current, the IBSMS generate the required MPPT duty cycle (u)(see Fig.3.). The IBSMC output command (u_{IBSMC}) includes two parts; equivalent integral backstepping (u) and discontinuous sliding mode (u_{dis}), as given in Eq.(5).

$$u_{IBSMC} = u + u_{dis} \tag{5}$$

Based on the IBSMC flowchart (Fig.4) , the error between the actual ($x_1 = I_{pv}$) and the MPPT required output PV current ($x_{1ref} = I_{pv-ref}$), is writing as:

$$\varepsilon_1 = x_1 - x_{1ref} \tag{6}$$

Our principal aim is to force this error to be zero. So and By deriving Eq. (6) and using Eq. (4), we obtain:

$$\dot{\varepsilon}_1 = \dot{x}_1 - \dot{x}_{1ref} = -\frac{(1-u)}{L}x_2 + \frac{V_{pv}}{L} - \dot{x}_{1ref} \tag{7}$$

The addition of the integral action of ε_1 the error term leads to:

$$e_1 = \varepsilon_1 + \zeta \tag{8}$$

With the integral term written as follows:

$$\zeta = \int_0^t (x_1 - x_{1ref})dt \tag{9}$$

In order to guarantee the convergence of the error (ε_1) to zero, the positive candidate of the Lyapunov function is chosen as:

$$V_1 = \frac{1}{2}\varepsilon_1^2 + \frac{1}{2}\kappa\zeta^2 \tag{10}$$

Where, κ is a positive definite real number which is needed to guarantee asymptotic system stability.This task is ensured if the time derivative of the Lyapunov function is always negative .The derivation of equation (10) gives:

$$\dot{V}_1 = \varepsilon_1\dot{\varepsilon}_1 + \kappa\zeta\dot{\zeta} \tag{11}$$

By using the time derivative of Eq. (9) and Eq. (7), we get:

$$\dot{V}_1 = \varepsilon_1\left(-\frac{(1-u)}{L}x_2 + \frac{V_{pv}}{L} - \dot{x}_{1ref}\right) + \kappa\zeta\left(x_1 - x_{1ref}\right) \tag{12}$$

The replacement of Eq. (6) in Eq. (12) permits to write:

$$\dot{V}_1 = \varepsilon_1 \left(-\frac{(1-u)}{L} x_2 + \frac{V_{pv}}{L} - \dot{x}_{1ref} + \kappa\zeta \right) \tag{13}$$

In order to guarantee the asymptotic system stability,$\dot{V}_1$ must be negative, the term $(-\frac{(1-u)}{L}x_2 + \frac{V_{pv}}{L} - \dot{x}_{1ref} + \kappa\zeta\ )$ in Eq. (13), is expressed by the following equation:

$$-\frac{(1-u)}{L} x_2 + \frac{V_{pv}}{L} - \dot{x}_{1ref} + \kappa\zeta = -k_1\varepsilon_1 \tag{14}$$

Where $k_1$is positive scalar. Therefore, $\dot{V}_1$ becomes:

$$\dot{V}_1 = -K_1\varepsilon_1^2 \tag{15}$$

Rewriting Eq. (14) as:

$$x_2 = \frac{L}{(1-u)} \left(\frac{V_{pv}}{L} - \dot{x}_{1ref} + \kappa\zeta + K_1\varepsilon_1 \right) \tag{16}$$

Whereas Eq.(16) is chosen as the reference voltage of the capacitor voltage , and is rewritten in the following form:

$$\lambda = \frac{L}{(1-u)} \left(\frac{V_{pv}}{L} - \dot{x}_{1ref} + \kappa\zeta + K_1\varepsilon_1 \right) \tag{17}$$

In order to guarantee the convergence of the actual value of the capacitor voltage (x_2) to its reference MPPT value (λ), a capacitor voltage error ε_2 is defined as follows:

$$\varepsilon_2 = x_2 - \lambda \tag{18}$$

Rewriting Eq. (17) as follow:

$$x_2 = \lambda + \varepsilon_2 \tag{19}$$

By Laying Eq. (7) in Eq. (19), we obtain:

$$\dot{\varepsilon}_1 = -\frac{(1-u)}{L} (\varepsilon_2 + \lambda) + \frac{V_{pv}}{L} - \dot{x}_{1ref} \tag{20}$$

The Replacement of λ from Eq. (17) in Eq. (20) gives:

$$\dot{\varepsilon}_1 = -\frac{(1-u)}{L} \varepsilon_2 - \kappa\zeta - k_1\varepsilon_1 \tag{21}$$

So, Eq. (11) can be rewritten as follow:

$$\dot{V}_1 = \varepsilon_1\dot{\varepsilon}_1 + \kappa\zeta\dot{\zeta} = -k_1\varepsilon_1^2 - \frac{\varepsilon_2\varepsilon_1\,(1-u)}{L} \tag{22}$$

The first term in Eq. (22) has always a negative definite form. However, we don't have any information about the second term form. By using the time derivative of Eqs. (17) and (18), we obtain respectively the following expressions:

$$\dot{\varepsilon}_2 = \dot{x}_2 - \dot{\lambda} \tag{23}$$

$$\dot{\lambda} = \frac{L}{(1-U)}\left(\frac{\dot{V}_{pv}}{L} - \ddot{x}_{1ref} + \kappa\dot{\zeta} + k_1\dot{\varepsilon}_1\right) - \frac{\dot{u}}{(1-u)^2}L\left(\frac{V_{pv}}{L} - \dot{x}_{1ref} + \kappa\zeta + K_1\varepsilon_1\right) \tag{24}$$

By using Eqs. (6), (9), (17), (21) for simplifying $\dot{\lambda}$, we get:

$$\dot{\lambda} = \frac{L}{(1-U)}\left(k_1\left(-\frac{(1-u)}{L}\varepsilon_2 - \kappa\zeta - K_1\varepsilon_1\right) + \frac{\dot{V}_{pv}}{L} - \ddot{x}_{1ref} + \kappa\varepsilon_1\right) - \frac{\dot{u}}{(1-u)}\lambda \tag{25}$$

Putting $\dot{\lambda}$ from Eq. (30) in Eq. (28), $\dot{\varepsilon_2}$ becomes:

$$\dot{\varepsilon}_2 = \dot{x}_2 - \frac{L}{(1-U)}\left(k_1\left(-\frac{(1-u)}{L}\varepsilon_2 - \kappa\zeta - K_1\varepsilon_1\right) + \frac{\dot{V}_{pv}}{L} - \ddot{x}_{1ref} + \kappa\varepsilon_1\right) - \frac{\dot{u}}{(1-u)}\lambda \tag{26}$$

In order to ensure convergence of both ε_2 and ε_1 to 0, a new composite Lyapunov function V_2 is defined, whose time derivative must be always negative in order to permit to the system to achieve the MPPT with a global stability guaranteed.

$$V_2 = V_1 + \frac{1}{2}\varepsilon_2^2 \tag{27}$$

Taking the derivative of Eq.(27) and using Eq.(22) we obtain:

$$\dot{V}_2 = \dot{V}_1 + \varepsilon_2\dot{\varepsilon}_2 = -k_1\varepsilon_1^2 - \frac{\varepsilon_2\varepsilon_1\,(1-u)}{L} + \varepsilon_2\dot{\varepsilon}_2 \tag{28}$$

$$\dot{V}_2 = \dot{V}_1 + \varepsilon_2\dot{\varepsilon}_2 = -k_1\varepsilon_1^2 + \varepsilon_2\left(\dot{\varepsilon}_2 - \frac{\varepsilon_1\,(1-u)}{L}\right) \tag{29}$$

To guarantee that $\dot{V}_2$ has a negative form, we pose:

$$\dot{\varepsilon}_2 - \frac{\varepsilon_1\,(1-u)}{L} = -k_2\varepsilon_1 \tag{30}$$

With K_2 is a positive scalar, so $\dot{V}_2$ becomes:

$$\dot{V}_2 = -k_1\varepsilon_1^2 - k_2\varepsilon_2^2 \tag{31}$$

Putting Eqs. (4) and (26) in (30), we obtain :

$$\frac{1}{L}x_1(1-u) - \frac{x_2}{RC} + k_1\varepsilon_1 + k_1\kappa\zeta\frac{L}{(1-u)} + k_1^2\varepsilon_1\frac{L}{(1-u)} - \frac{\dot{V}_{pv}}{(1-u)} + (\ddot{x}_{1ref} - \varepsilon_1)\frac{L}{(1-u)} + \frac{\dot{u}}{(1-u)}\lambda - \varepsilon_1\frac{(1-u)}{L} = -k_2\varepsilon_2 \tag{32}$$

From Eq. (32), one can write:

$$\dot{u} = \frac{(1-u)}{\lambda}\left(\varepsilon_1\frac{(1-u)}{L}\right) + \frac{(1-u)}{\lambda}\left(-\frac{Lk_1\kappa\zeta}{(1-u)} - \frac{k_1^2\varepsilon_1 L}{(1-u)} + \varepsilon_1\frac{L}{(1-u)} - \frac{L}{(1-u)}\ddot{x}_{1ref}\right) + \frac{(1-u)}{\lambda}\left(\frac{\dot{V}_{pv}}{L} + \varepsilon_1\frac{(1-u)}{L}\right) + \frac{(1-u)}{\lambda}\left(-k_2\varepsilon_2 - \frac{1}{L}x_1(1-u) + \frac{x_2}{RC} - k_1\varepsilon_2\right) \tag{33}$$

Where $\lambda \neq 0$ and $u \in [0, 1]$.

The integration of this last equation gives the required MPPT duty cycle value (u) (equivalent IBS command in Eq (5)). Since the boost duty cycle command (Eq(**??**)) is calculated based on Lyapunov criteria, the global system stability is always ensured.

3.4. Discontinuous Sliding mode control

In this section, the discontinuous sliding mode term (u_{dis}) in Eq(5) is determined. The surface of sliding is considered as follow:

$$S = e_1 = \varepsilon_1 + \zeta \tag{34}$$

The main objective of using the discontinuous controller is to reduce the chattering ripples, in the case of considering the external disturbances. The discontinuous sliding mode control law can be written as follows[29]:

$$u_{dis} = -k_3\frac{S}{|S| + \delta} \tag{35}$$

Where k_3 is a large constant value which is chosen to ensure the system stability condition and δ is a small positive number which is designed using results of simulation and experiments, in order to reduce the chattering phenomena effect. Finally by adding Eq. (35) to the integration of the Eq. (**??**, the proposed integral backstepping sliding mode control output is given by:

$$u_{IBSMC} = u + u_{dis} \tag{36}$$

4. Classical sliding mode

In order to compare the performances of the proposed IBSMC and the classical sliding mode in terms of state error minimization and chattering phenomena reduction, this section is dedicated to describing briefly the structure a classical sliding mode controller. In this work, we have chosen to use a sliding mode strategy developed in [20]. Authors have proposed a simple sliding mode approach to achieve the maximum power point for the PV array. The different principal equations of this approach are given as follows:

$$S_1 = \varepsilon_1 = x_1 - x_{1ref} \tag{37}$$

$$u_1 = \frac{1}{2}(1 + Sign(S_1)) \tag{38}$$

$$u_1 = \left\{ \begin{array}{ll} 1 & if \quad S_1 > 0 \\ 0 & if \quad S_1 < 0 \end{array} \right\} \tag{39}$$

Where S_1 is the sliding surface and u is the signal control of the boost converter. The stability of this controller is analyzed based on the Lyapunov criteria in[20].

5. Simulation results and discussions

In order to prove the performances of the proposed controller, Matlab / SIMULINK is used to perform the system dynamic responses. Our main objective is to analyze and compare the performances of two nonlinear controllers (IBSMC and classical SMC) in order to track the MPP of PV panel under the same conditions of the weather. The studied system consists of a boost converter circuit feeding a resistor load. A PV panel that contains commercial PV modules "$BISOLPV Monocrystalline/BMO300Wc$"whose parameters panel are mentioned in Table.1.Moreover, Table.2 summarized the IBSMC controller parameters and the boost converter design. In order to compare the performances of the two controllers for MPP searching, two cases of the irradiation are considered ($1000W/m^2$and $728W/m^2$) with a fixed temperature value of $25C^0$ (see Table 2). This simulation tests have been preformed to evaluate the ability and robustness of the proposed controller under fast irradiation condition changing.

Table 1: Parameters of PV module

Module Parameters	Value
Power at MPP $P_{mpp}(W)$	300
short circuit current $I_{cc}(A)$	9.75
voltage at MPP $V_{mpp}(V)$	31.9
current at MPP $I_{mpp}(V)$	9.40
open circuit voltage $V_{co}(A)$	39.8
module yield η_M [%]	18,4

Table 2: Parameters of boost converter and controller

parameter	value
$k1$	700
$k2$	8240.65
$k3$	0.01
k	1207
δ	0.5
Inductor,L	1 mH
Capacitor, $C1$	200 μF
capacitor , $C2$	2200 μF
load resistor,R	12 Ω

Fig.6 shows the $I-V$ and $P-V$ characteristics of the PV module with a fixed temperature and the two considered irradiation values.

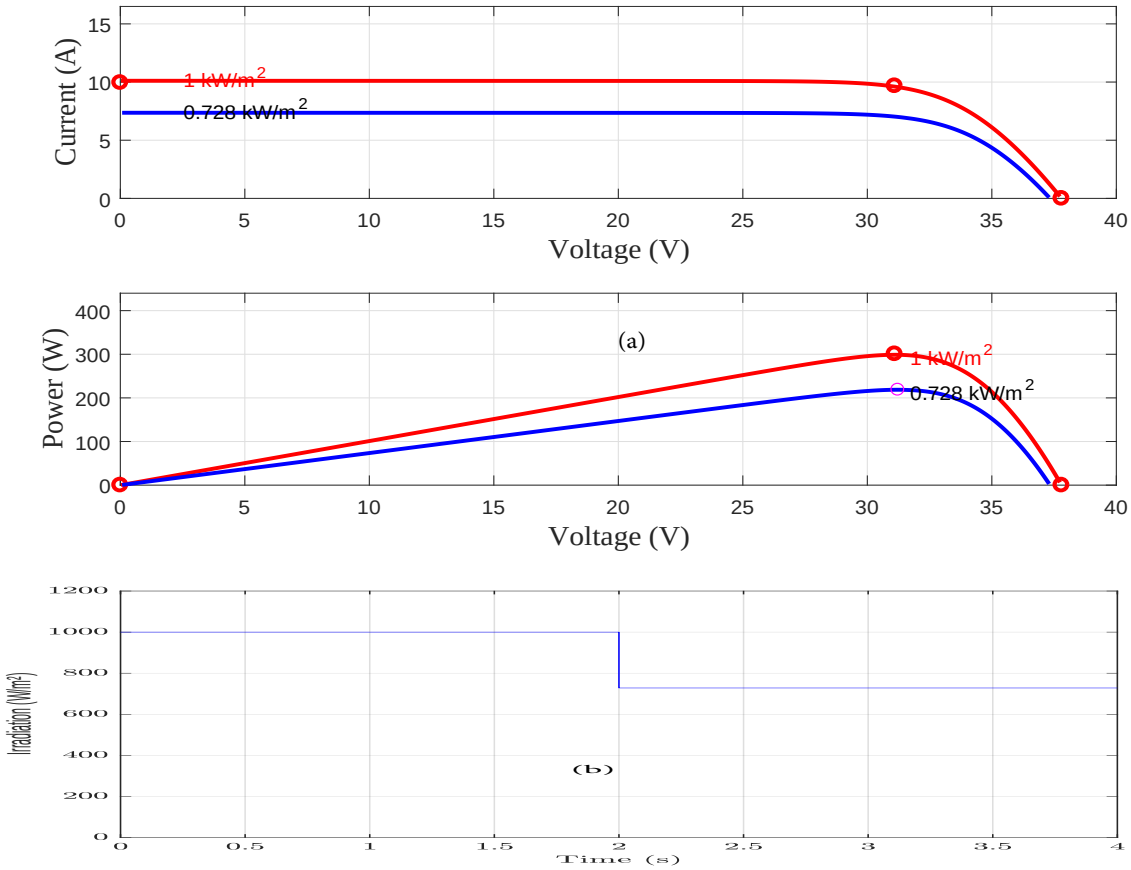

Figure 6: a) PV module characteristics, b) Irradiation (W/m^2).

In order to perform a comparison between IBSMC and SMC performances, the PV-current, PV-voltages, PV-power and load-power responses are considered. State error and chattering ripples are taken as a key factor to judge the goodness of the proposed controller. The obtained simulation results are shown in Fig.(7 and 8). From these figures, one can remark clearly that IBSMC has better dynamic performances comparatively to those of SMC. Moreover, from the zoomed figure of the PV-power (Fig.7(c)), the chattering phenomena and the state error have been reduced considerably in the case of using IBSMC. Practically, these improved performances are due essentially to the integral action and the discontinuous sliding mode controller integrated into the IBSMC structure. Indeed, the discontinuous sliding mode law affects clearly the chattering ripples that improve clearly the power quality and by the way ensure the stability of the overall system. The integral action has enhanced state error.

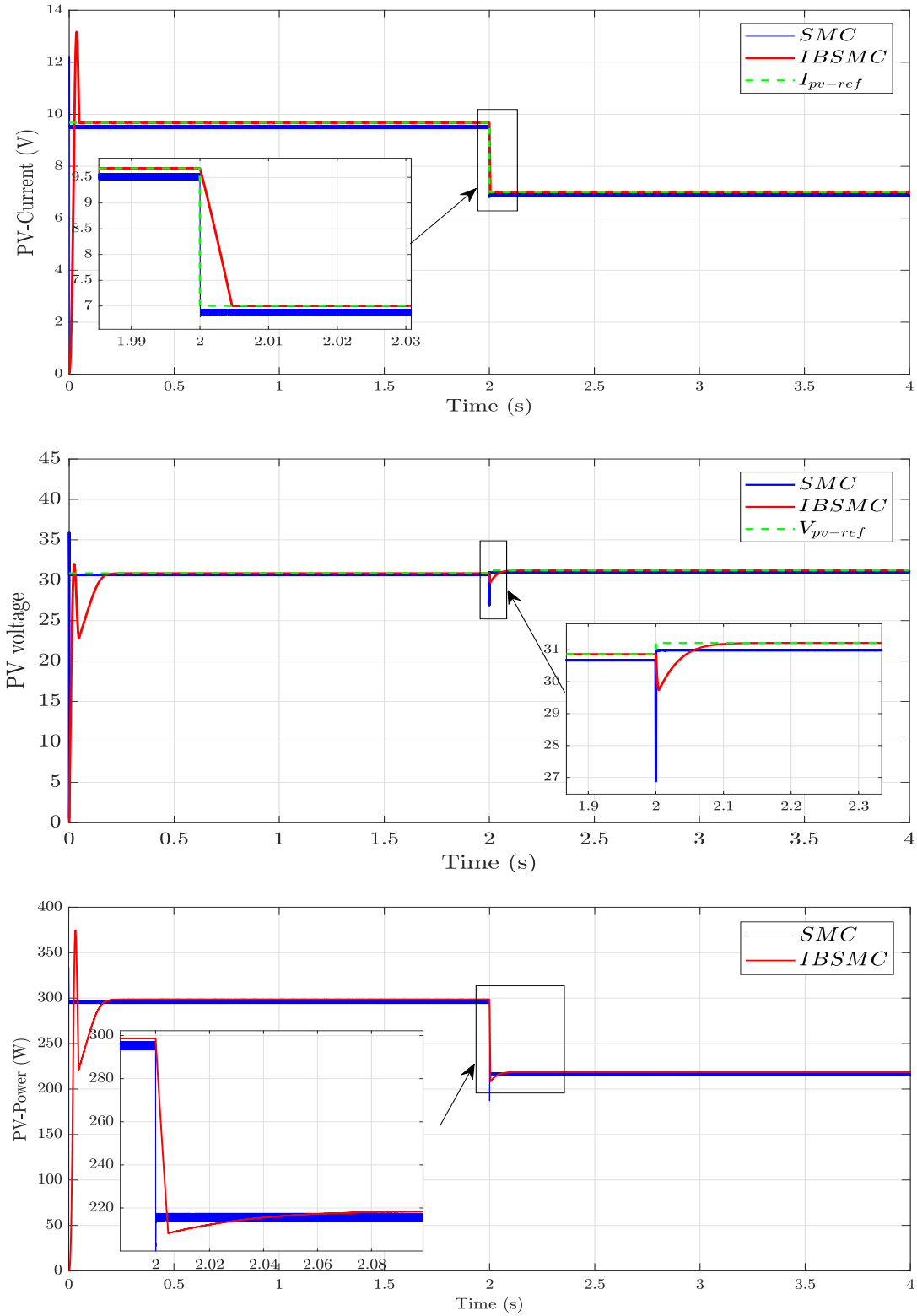

Figure 7: Different responses of the PV module in the case of IBSMC and SMC: a) PV- current (A), b) PV-voltage (V), c) PV-power (W).

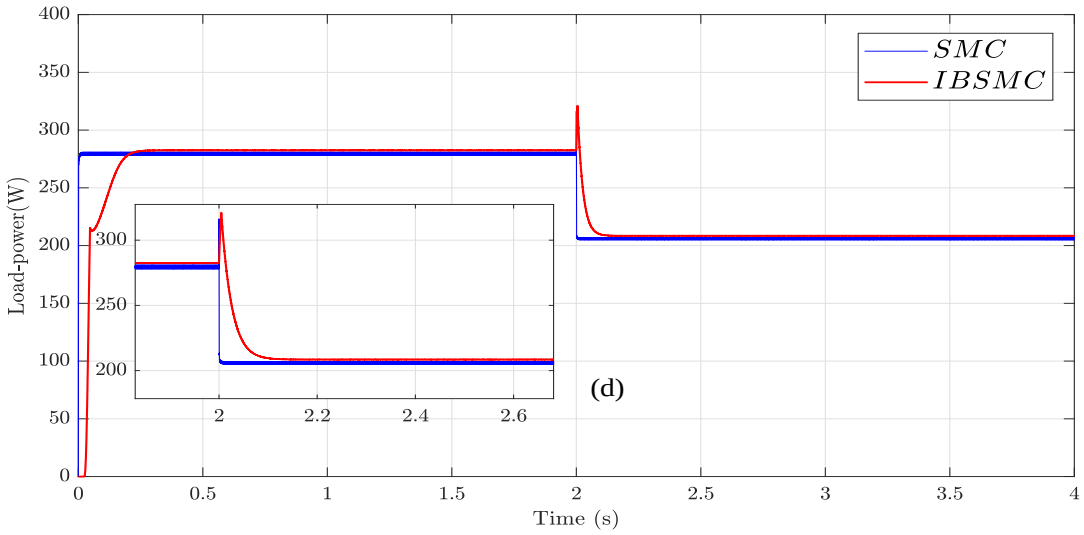

Figure 8: Load-power(W) of the PV module in the case of IBSMC

6. Experimental results and discussions

The experimental results are carried out on the basis of test bench existing in our laboratory.As shown in Fig.9. The list of material used in the experience is given hereafter:

- dSPACE (Dsp1 and Dsp 2);
- Variable resistive loads (load1 and load 2);
- Voltage and current sensors;
- DC-DC Boost converters (boost 1 and boost 2);
- Two PV modules (PV1 and PV2) (see Fig.9);
- Graphical User Interface (GUI1 and GUI2);
- Device for PV module characteristics measurement (see Figs.10).

Figure 9: Different required devices used for practical experience.

Figure 10: Device for PV module characteristics measurement.

6.1. Experimental measurement of the PV module characteristics

6.2. Case of constant weather conditions

The device, shown in 10, is used for the PV module characteristics measurement for irradiation of about $728W/m^2$ generated by an irradiation sensor available in the laboratory (see Fig.11). The obtained experimental PV characteristics ($I-V$ and $P-V$) for irradiation of ($728W/m^2$) and a temperature of about $26C^0$ are presented in Fig 12. From these results, the practical maximum PV power which can be produced for the actual irradiation value ($728W/m^2$) is about equal to $215.4(W)$ for a PV voltage and current equal to $29.89V$ and $7.2A$ respectively (see Fig.11).

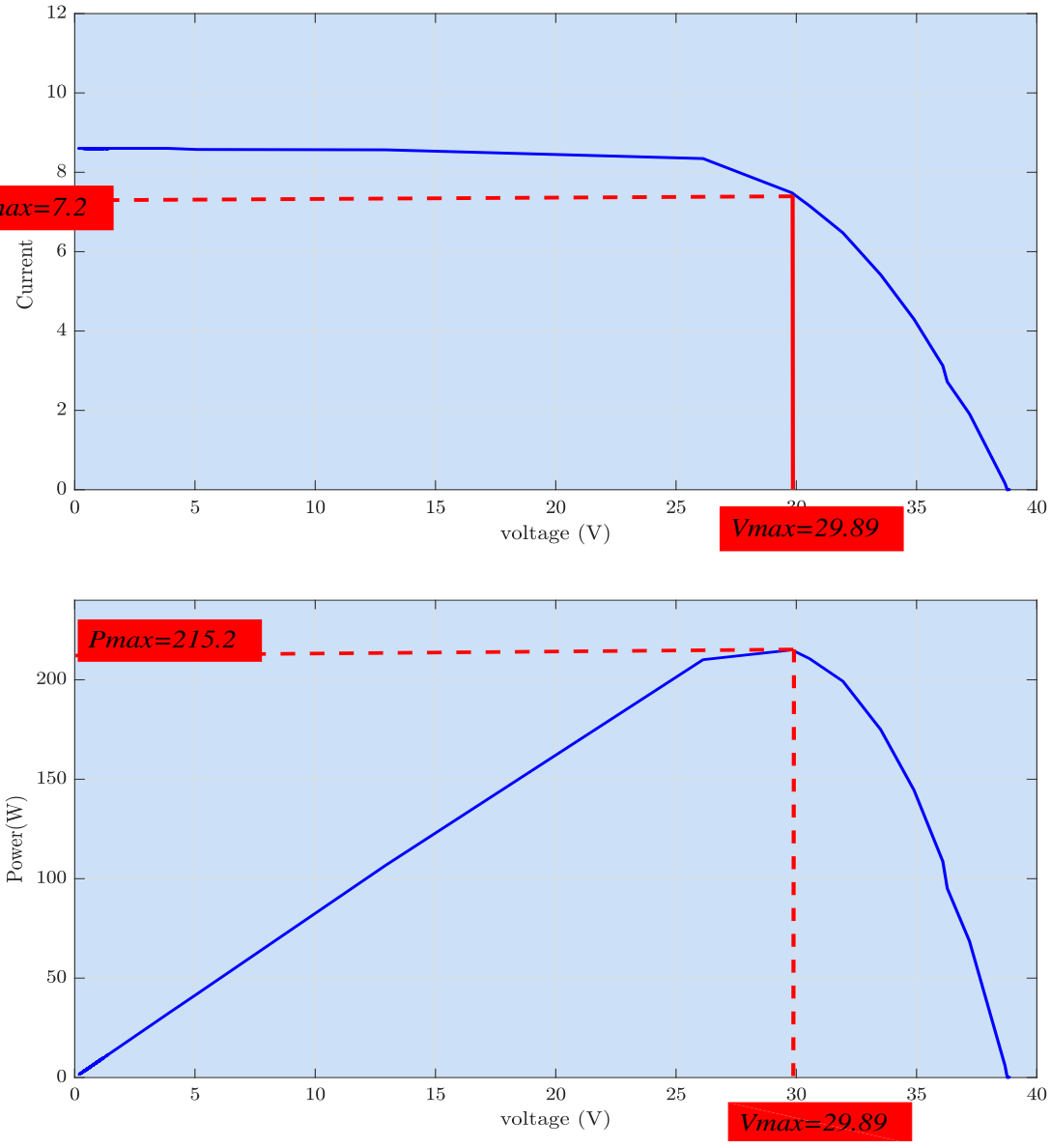

Figure 11: Experimental PV characteristics ($I-V$ and $P-V$) at an irradiation of $728w/m2$.

In addition, the experimental irradiation curve given by the sensor is presented in Fig.12.

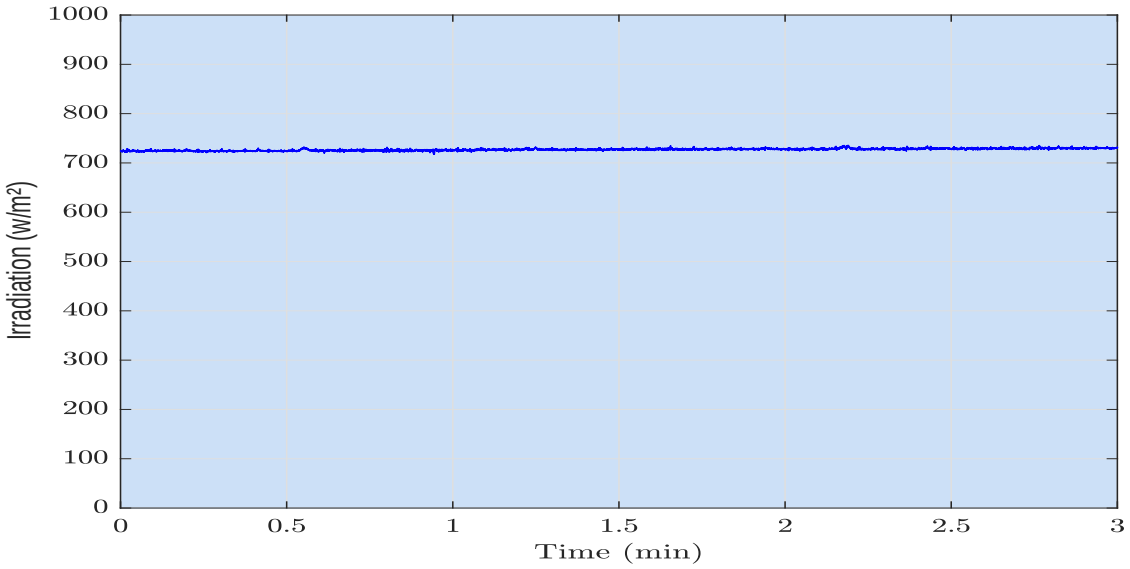

Figure 12: Experimental irradiation curve (W/m^2).

6.3. Experimental results using the controllers

The controller's strategies developed previously are applied practically to the PV system. The IBSMC and SMC are tuned at the same time to control the PV current to follow its MPPT value and achieve consequently the maximum produced power. The different experimental PV responses are shown in Fig.13. The experimental results show that all different PV responses ($PV-voltage$, $PV-current$ and $PV-power$) are following practically their MPPT values by applying the two controllers with the same weather practical conditions (irradiation and temperature).However, in the case of the IBSMC, the state error and the chattering phenomena are reduced considerably (see Fig.13 (b and c)). As a result, a smooth PV power form (very small chattering level) is achieved by the use of the IBSMC (see Fig.13(c)). Elsewhere, the experimental load responses are depicted in Fig.14. From these results, one can remark that all load responses ($load-current$,$load-voltage$, $load-power$) follow their MPPT required values. In the case of using SMC, all the practical responses contain the chattering phenomena with a non nil state error, but these drawbacks are significantly reduced in the case of IBSMC (see Fig.14 (b and c)). In fact, a smooth load voltage and power are guaranteed for feeding the load. So, by using the IBSMC the power quality is suitably enhanced . Finally, comparing the curves of the PV- power(see Fig.13(c)) and

the $load - power$(see Fig.14(c)) , one can observe a little difference which is due to the system losses.

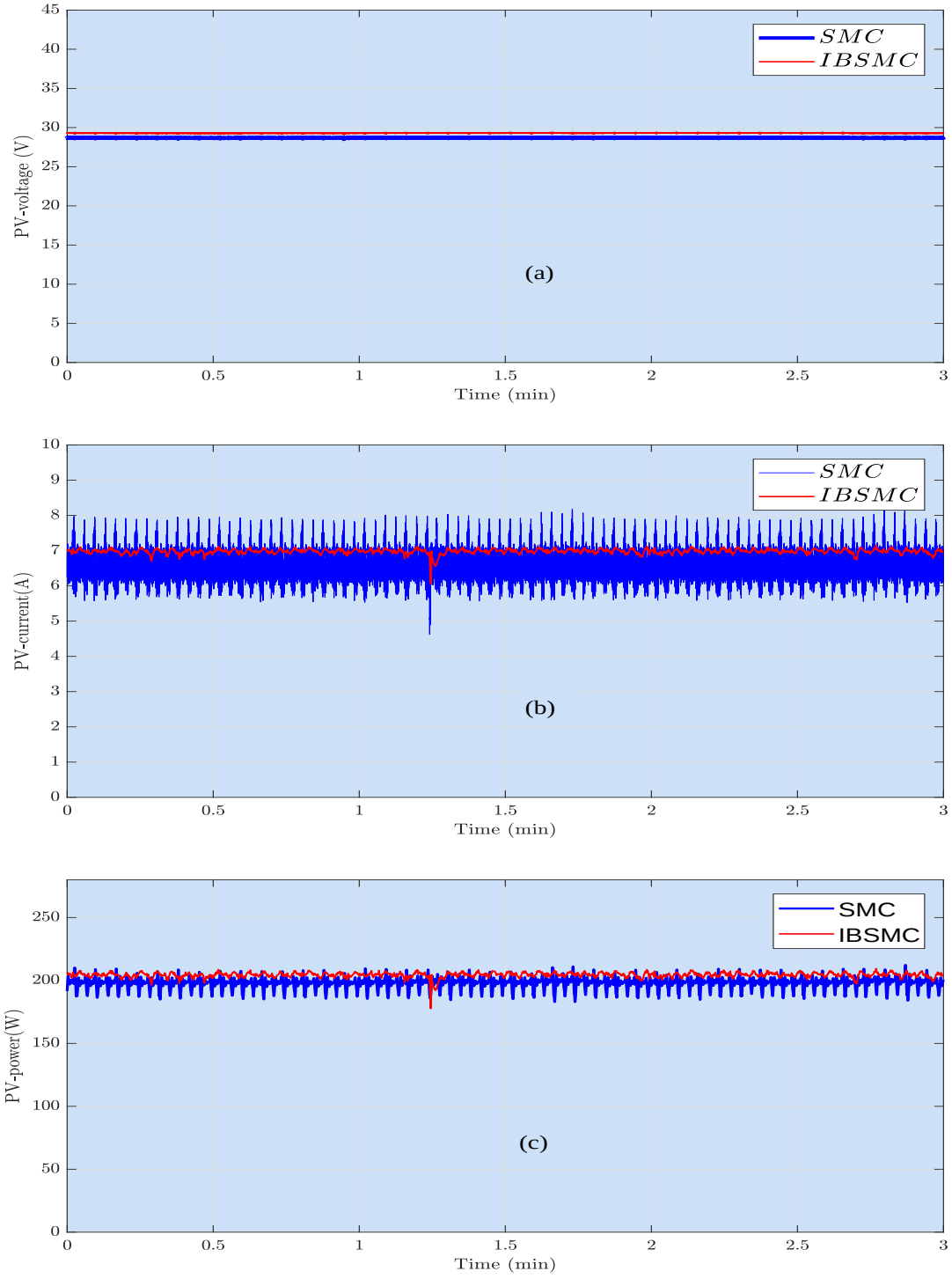

Figure 13: Different experimental responses of the PV module in the case of IBSMC and SMC: a) PV-voltage (V), b) PV-current (A), c) PV-power (W).

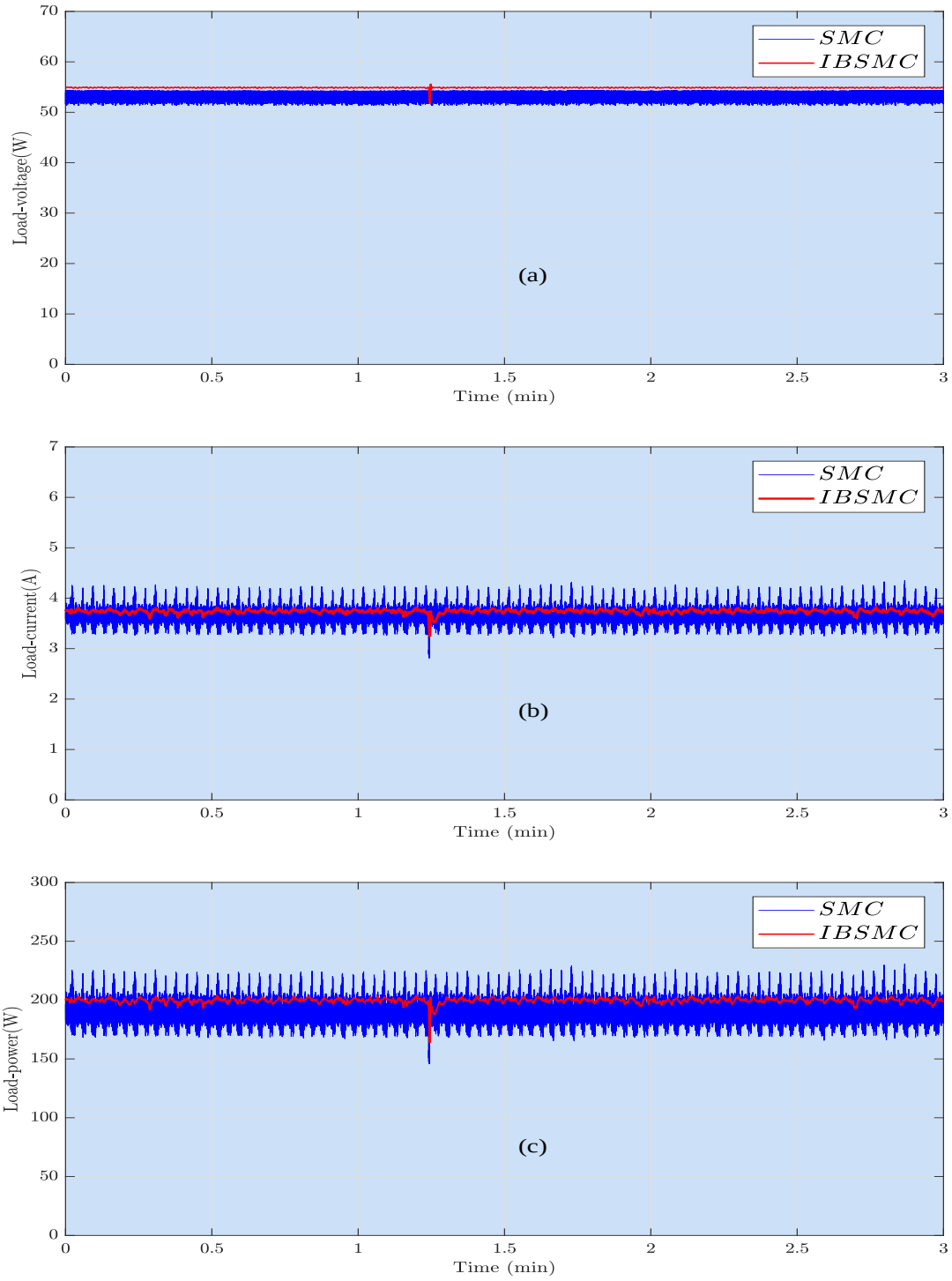

Figure 14: Different experimental responses of the load in the case of IBSMC and SMC: a) Load-voltage (V), b) Load-current (V), c) Load-power (W).

Finally, to show clearly the performances of the proposed controller, the obtained load power is measured through an oscilloscope and presented in Fig.16. The use of the IBSMC leads to an

improved power quality (smooth power curve).(see Fig.16)

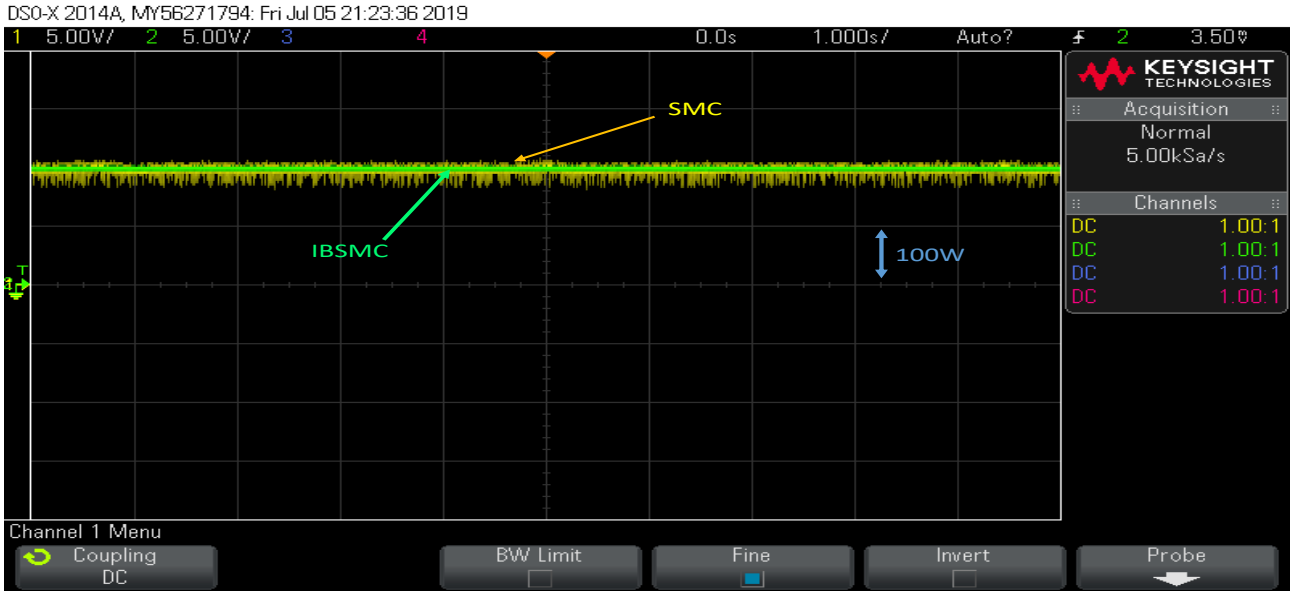

Figure 15: Load power measurement of the load power in the case of the IBSMC and the SMC.

6.4. Case of variable weather conditions

As a second test, the experiments were carried out by considering a large change in weather conditions (Duration of 4 hours) in a very cloudy day. To evaluate the performances of the proposed controller (IBSMC) in term of robustness, global stability and tracking the reference value. A comparison between SMC and IBSMC has been made in real-time under the same irradiation and temperature. The obtained experimental results for both controllers are shown in Fig 16. It can be seen that the use the proposed IBSMC controller allow, a great improvement of the load power quality, a high reduction of the chattering phenomenon and minimize the steady state-error.

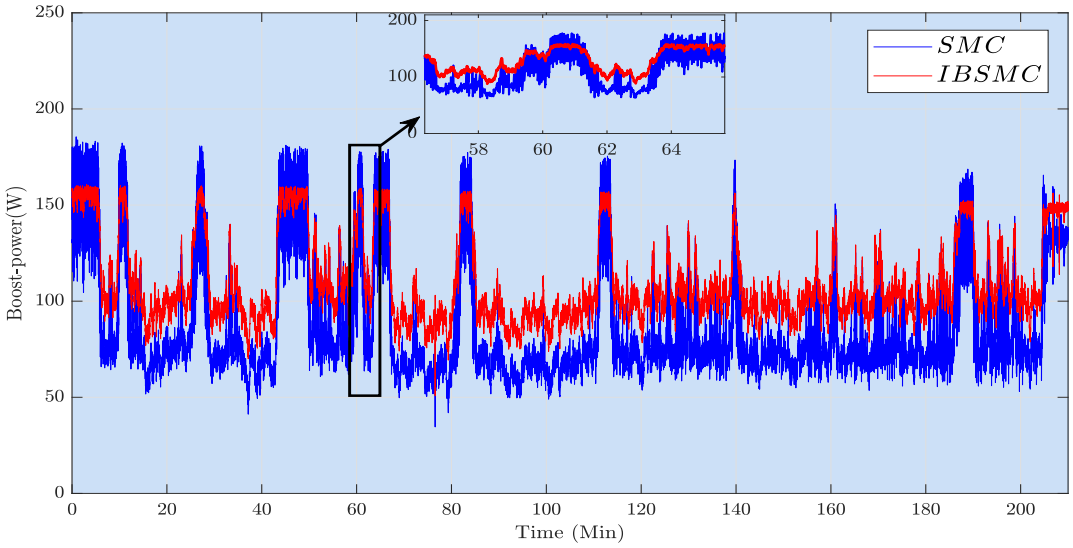

Figure 16: Experimental load (Boost-power (W)).responses in the case of IBSMC and SMC under large variable weather conditions.

7. Conclusion

Nonlinear controllers are the most suitable for PV systems control. In this paper, a nonlinear Integral Backstepping Sliding Mode Controller (IBSMC) to achieve the PV MPP using DC-DC boost converter had been proposed. The current reference value at the MPP has been generated using a classical method (P&O) and the global stability of the system has been improved using Lyapunov stability criteria. The IBSMC controller is based on a combination of a discontinuous sliding mode and an integral backstepping to reduce simultaneously the chattering phenomena and minimize the steady-state error. The performances of the proposed controller have been applied and tested through simulations and experimental validation using a test bench. Furthermore, its performances have been compared experimentally with a nonlinear classical Sliding mode controller under the same weather conditions. The obtained experimental results demonstrate an improved steady-state error and chattering phenomena minimization, using the proposed controller. So, the MPP tracking is accurately achieved and the system power quality is suitably enhanced.

Future work can be focused on the test experimentally the IBSMC performances under partial shading conditions and improving the system response time by optimizing the IBSMC controller parameters using optimization technique .

References

[1] T. Poompavai, M. Kowsalya, Control and energy management strategies applied for solar photovoltaic and wind energy fed water pumping system: A review, Renewable and Sustainable Energy Reviews 107 (2019) 108–122. doi:10.1016/j.rser.2019.02.023.
URL https://linkinghub.elsevier.com/retrieve/pii/S1364032119301169

[2] R. Ahmad, A. F. Murtaza, H. A. Sher, Power tracking techniques for efficient operation of photovoltaic array in solar applications – A review, Renewable and Sustainable Energy Reviews 101 (2019) 82–102. doi:10.1016/j.rser.2018.10.015.
URL https://linkinghub.elsevier.com/retrieve/pii/S1364032118307196

[3] D. Sera, L. Mathe, T. Kerekes, S. V. Spataru, R. Teodorescu, On the Perturb-and-Observe and Incremental Conductance MPPT Methods for PV Systems, IEEE Journal of Photovoltaics 3 (3) (2013) 1070–1078. doi:10.1109/JPHOTOV.2013.2261118.
URL http://ieeexplore.ieee.org/document/6517453/

[4] R. Alik, A. Jusoh, An enhanced P&O checking algorithm MPPT for high tracking efficiency of partially shaded PV module, Solar Energy 163 (2018) 570–580. doi:10.1016/j.solener.2017.12.050.
URL https://linkinghub.elsevier.com/retrieve/pii/S0038092X17311325

[5] B. K. Oubbati, M. Boutoubat, M. Belkheiri, A. Rabhi, Extremum Seeking and P&O Control Strategies for Achieving the Maximum Power for a PV Array, in: M. Hatti (Ed.), Renewable Energy for Smart and Sustainable Cities, Vol. 62, Springer International Publishing, Cham, 2019, pp. 233–241. doi:10.1007/978-3-030-04789-4_26.
URL http://link.springer.com/10.1007/978-3-030-04789-4_26

[6] A. M. Eltamaly, H. M. Farh, Dynamic global maximum power point tracking of the PV systems under variant partial shading using hybrid GWO-FLC, Solar Energy 177 (2019) 306–316. doi:10.1016/j.solener.2018.11.028.
URL https://linkinghub.elsevier.com/retrieve/pii/S0038092X18311290

[7] H. Hamdi, C. Ben Regaya, A. Zaafouri, Real-time study of a photovoltaic system with boost converter using the PSO-RBF neural network algorithms in a MyRio controller, Solar Energy

183 (2019) 1–16. doi:10.1016/j.solener.2019.02.064.
URL https://linkinghub.elsevier.com/retrieve/pii/S0038092X19301902

[8] M. A. Mohamed, A. A. Zaki Diab, H. Rezk, Partial shading mitigation of PV systems via different meta-heuristic techniques, Renewable Energy 130 (2019) 1159–1175. doi:10.1016/j.renene.2018.08.077.
URL https://linkinghub.elsevier.com/retrieve/pii/S0960148118310279

[9] B. Yang, L. Zhong, X. Zhang, H. Shu, T. Yu, H. Li, L. Jiang, L. Sun, Novel bio-inspired memetic salp swarm algorithm and application to MPPT for PV systems considering partial shading condition, Journal of Cleaner Production 215 (2019) 1203–1222. doi:10.1016/j.jclepro.2019.01.150.
URL https://linkinghub.elsevier.com/retrieve/pii/S0959652619301696

[10] M. Mao, L. Zhou, Z. Yang, Q. Zhang, C. Zheng, B. Xie, Y. Wan, A hybrid intelligent GMPPT algorithm for partial shading PV system, Control Engineering Practice 83 (2019) 108–115. doi:10.1016/j.conengprac.2018.10.013.
URL https://linkinghub.elsevier.com/retrieve/pii/S0967066118306592

[11] A. Mohapatra, B. Nayak, P. Das, K. B. Mohanty, A review on MPPT techniques of PV system under partial shading condition, Renewable and Sustainable Energy Reviews 80 (2017) 854–867. doi:10.1016/j.rser.2017.05.083.
URL https://linkinghub.elsevier.com/retrieve/pii/S1364032117307256

[12] M. Seyedmahmoudian, B. Horan, T. K. Soon, R. Rahmani, A. M. Than Oo, S. Mekhilef, A. Stojcevski, State of the art artificial intelligence-based MPPT techniques for mitigating partial shading effects on PV systems – A review, Renewable and Sustainable Energy Reviews 64 (2016) 435–455. doi:10.1016/j.rser.2016.06.053.
URL https://linkinghub.elsevier.com/retrieve/pii/S1364032116302842

[13] H. M. El-Helw, A. Magdy, M. I. Marei, A Hybrid Maximum Power Point Tracking Technique for Partially Shaded Photovoltaic Arrays, IEEE Access 5 (2017) 11900–11908. doi:10.1109/ACCESS.2017.2717540.
URL http://ieeexplore.ieee.org/document/7953645/

[14] B. K. Oubbati, M. Boutoubat, M. Belkheiri, A. Rabhi, Global maximum power point tracking of a PV system MPPT control under partial shading, in: 2018 International Conference on Electrical Sciences and Technologies in Maghreb (CISTEM), IEEE, Algiers, 2018, pp. 1–6. doi:10.1109/CISTEM.2018.8613391.
URL https://ieeexplore.ieee.org/document/8613391/

[15] A. El Khateb, N. A. Rahim, J. Selvaraj, M. N. Uddin, Fuzzy-Logic-Controller-Based SEPIC Converter for Maximum Power Point Tracking, IEEE Transactions on Industry Applications 50 (4) (2014) 2349–2358. doi:10.1109/TIA.2014.2298558.
URL http://ieeexplore.ieee.org/document/6704722/

[16] K. Ishaque, Z. Salam, A review of maximum power point tracking techniques of PV system for uniform insolation and partial shading condition, Renewable and Sustainable Energy Reviews 19 (2013) 475–488. doi:10.1016/j.rser.2012.11.032.
URL https://linkinghub.elsevier.com/retrieve/pii/S1364032112006442

[17] P. Verma, R. Garg, P. Mahajan, Asymmetrical interval type-2 fuzzy logic control based MPPT tuning for PV system under partial shading condition, ISA Transactions (2020) S0019057820300021doi:10.1016/j.isatra.2020.01.009.
URL https://linkinghub.elsevier.com/retrieve/pii/S0019057820300021

[18] R. Abdelrassoul, Y. Ali, M. S. Zaghloul, Genetic Algorithm-Optimized PID Controller for Better Performance of PV System, in: 2016 World Symposium on Computer Applications & Research (WSCAR), IEEE, Cairo, Egypt, 2016, pp. 18–22. doi:10.1109/WSCAR.2016.14.
URL http://ieeexplore.ieee.org/document/7791974/

[19] E. K. Anto, J. A. Asumadu, P. Y. Okyere, PID control for improving P&O-MPPT performance of a grid-connected solar PV system with Ziegler-Nichols tuning method, in: 2016 IEEE 11th Conference on Industrial Electronics and Applications (ICIEA), IEEE, Hefei, China, 2016, pp. 1847–1852. doi:10.1109/ICIEA.2016.7603888.
URL http://ieeexplore.ieee.org/document/7603888/

[20] M. Farhat, O. Barambones, L. Sbita, A new maximum power point method based on a sliding mode approach for solar energy harvesting, Applied Energy 185 (2017) 1185–1198.

doi:10.1016/j.apenergy.2016.03.055.
URL https://linkinghub.elsevier.com/retrieve/pii/S0306261916303750

[21] M. Bjaoui, B. Khiari, R. Benadli, M. Memni, A. Sellami, Practical Implementation of the Backstepping Sliding Mode Controller MPPT for a PV-Storage Application, Energies 12 (18) (2019) 3539. doi:10.3390/en12183539.
URL https://www.mdpi.com/1996-1073/12/18/3539

[22] K. Dahech, M. Allouche, T. Damak, F. Tadeo, Backstepping sliding mode control for maximum power point tracking of a photovoltaic system, Electric Power Systems Research 143 (2017) 182–188. doi:10.1016/j.epsr.2016.10.043.
URL https://linkinghub.elsevier.com/retrieve/pii/S0378779616304400

[23] Naghmash, H. Armghan, I. Ahmad, A. Armghan, S. Khan, M. Arsalan, Backstepping based non-linear control for maximum power point tracking in photovoltaic system, Solar Energy 159 (2018) 134–141. doi:10.1016/j.solener.2017.10.062.
URL https://linkinghub.elsevier.com/retrieve/pii/S0038092X17309428

[24] R. Pradhan, B. Subudhi, Double Integral Sliding Mode MPPT Control of a Photovoltaic System, IEEE Transactions on Control Systems Technology 24 (1) (2016) 285–292. doi:10.1109/TCST.2015.2420674.
URL http://ieeexplore.ieee.org/document/7101232/

[25] B. Yang, T. Yu, H. Shu, D. Zhu, N. An, Y. Sang, L. Jiang, Perturbation observer based fractional-order sliding-mode controller for MPPT of grid-connected PV inverters: Design and real-time implementation, Control Engineering Practice 79 (2018) 105–125. doi:10.1016/j.conengprac.2018.07.007.
URL https://linkinghub.elsevier.com/retrieve/pii/S096706611830279X

[26] M. Stitou, A. E. Fadili, F. Z. Chaoui, F. Giri, Output feedback control of sensorless photovoltaic systems, with maximum power point tracking, Control Engineering Practice 84 (2019) 1–12. doi:10.1016/j.conengprac.2018.10.020.
URL https://linkinghub.elsevier.com/retrieve/pii/S0967066118302922

[27] R. Chinnappan, P. Logamani, R. Ramasubbu, Fixed frequency integral sliding-mode current-controlled MPPT boost converter for two-stage PV generation system, IET Circuits, Devices

& Systems 13 (6) (2019) 793–805. doi:10.1049/iet-cds.2018.5221.
URL https://digital-library.theiet.org/content/journals/10.1049/iet-cds.2018.5221

[28] N. Chatrenour, H. Razmi, H. Doagou-Mojarrad, Improved double integral sliding mode MPPT controller based parameter estimation for a stand-alone photovoltaic system, Energy Conversion and Management 139 (2017) 97–109. doi:10.1016/j.enconman.2017.02.055.
URL https://linkinghub.elsevier.com/retrieve/pii/S0196890417301668

[29] A. Kihal, F. Krim, A. Laib, B. Talbi, H. Afghoul, An improved MPPT scheme employing adaptive integral derivative sliding mode control for photovoltaic systems under fast irradiation changes, ISA Transactions 87 (2019) 297–306. doi:10.1016/j.isatra.2018.11.020.
URL https://linkinghub.elsevier.com/retrieve/pii/S0019057818304555

[30] M. Arsalan, R. Iftikhar, I. Ahmad, A. Hasan, K. Sabahat, A. Javeria, MPPT for photovoltaic system using nonlinear backstepping controller with integral action, Solar Energy 170 (2018) 192–200. doi:10.1016/j.solener.2018.04.061.
URL https://linkinghub.elsevier.com/retrieve/pii/S0038092X18304274

[31] A. Oi, M. Anwari, M. Taufik, Modeling and Simulation of Photovoltaic Water Pumping System, in: 2009 Third Asia International Conference on Modelling & Simulation, IEEE, Bundang, Bali, Indonesia, 2009, pp. 497–502. doi:10.1109/AMS.2009.85.
URL http://ieeexplore.ieee.org/document/5072037/

[32] E. Van Dijk, J. Spruijt, D. O'Sullivan, J. Klaassens, PWM-switch modeling of DC-DC converters, IEEE Transactions on Power Electronics 10 (6) (1995) 659–665. doi:10.1109/63.471285.
URL https://ieeexplore.ieee.org/document/471285/